

FIBRE-OPTIC COMMUNICATION LINES

DOI: 10.1070/QE2016v046n01ABEH015841

Numerical modelling of multimode fibre-optic communication lines

O.S. Sidelnikov, S. Sygletos, F. Ferreira, M.P. Fedoruk

Abstract. **The results of numerical modelling of nonlinear propagation of an optical signal in multimode fibres with a small differential group delay are presented. It is found that the dependence of the error vector magnitude (EVM) on the differential group delay can be reduced by increasing the number of ADC samples per symbol in the numerical implementation of the differential group delay compensation algorithm in the receiver. The possibility of using multimode fibres with a small differential group delay for data transmission in modern digital communication systems is demonstrated. It is shown that with increasing number of modes the strong coupling regime provides a lower EVM level than the weak coupling one.**

Keywords: *multimode fibre, differential group delay, mathematical modelling, Manakov equation.*

1. Introduction

Today more than 99% of global information flows are processed using fibre-optic communication systems. Fibre-optic communication lines offer the most efficient solution for transferring large amounts of data over large distances. An exponentially growing demand for the transmission capacity of communication lines stimulates the studies in the field of high-power optical data transmission systems. Using the coherent detection, autonomous signal processing and the 128-QAM modulation format, the transmission rate of 101.7 Tbit s^{-1} was achieved with the spectral efficiency 11 bit s^{-1} Hz^{-1} in the transmission over three spans 55 km long with Raman amplification of the signals [1]. As shown by recent experiments, using a fibre with a low nonlinearity level and high-efficiency methods of digital signal processing, one can transfer data with the rate 400 Gbit s^{-1} over the distance exceeding 12000 km with 100 GHz channel spacing [2]. The studies carried out at present and aimed at a further increase in the transmission capacity in a standard single-mode fibre [3, 4] face difficulties related to the limitations of the operating range of fibre amplifiers, severe requirements to the signal-to-noise ratio and the limited power of the fibre input signal. The annual traffic growth already exceeds the growth of the transmission capacity, and in the nearest years, we may face the problem of the traffic volume exceeding the capabilities of data transmission technologies, if no new technology, providing a significant increase in the transmission capacity of communication lines, will be offered.

The development of communication systems based on multimode fibres is considered as a promising way for solving the above problem [5, 6]. Multimode fibres allow an increase in the transmission capacity of optical networks at the expense of simultaneous transmission of signals via multiple modes of the fibre. Moreover, these fibres have the following advantages. Their core diameter is a few times larger than in the single-mode fibres, which is convenient in the process of mounting. A multimode cable can be simpler provided with terminal fibre connectors having low losses (to 0.3 dB) at the connection. Finally, the emitters generating at the wavelength 0.85 μm, which are the most available and cheap radiation sources produced in broad assortment, are specially designed for multimode fibres. The method of signal transmission using different spatial modes of the optical fibre is referred to as the space-division multiplexing (SDM). By means of wavelength-division multiplexing (WDM), time-division multiplexing (TDM), polarisation-division multiplexing (PDM) and forward error correction (FEC) in the multimode fibre the data transmission rates from 100 Tbit s^{-1} to 1 Pbit s^{-1} were achieved [7–9]. The use of Multiple Input Multiple Output (MIMO) technology in such fibres made available the transmission of data with a high speed over large distances [10]. Based on multimode fibres the high-efficiency high-power fibre Raman lasers are developed [11]. Besides, these fibres have found wide applications in biomedicine as the basis for manufacturing biosensors [12] and in optics for fabrication of interferometers [13]. Multimode fibres are widely introduced into local networks, replacing single-mode ones [14].

However, when the data are transmitted over large distances using a multimode fibre, a number of problems arise. One of them is the difficulty of signal equalising in the course of its detection in the receiver [15]. The signals transmitted by different modes of the fibre propagate with different velocities, so that before the signal detection in the receiver the equaliser must receive and store the signals of faster modes until the slowest mode signal arrives. Two approaches exist to the reduction of the differential group delay (DGD) of the fibre in order to soften the requirement to the MIMO equaliser memory: to use fibres with a low DGD [16] or fibres with a compensated differential group delay, consisting of alternating segments with the opposite sign of the DGD [17].

In the case of fibres with the compensated differential group delay, the welding problems arise. Therefore, for simplicity of further use we have decided to consider a multimode fibre with a low value of the DGD. In the present paper, we

O.S. Sidelnikov, M.P. Fedoruk Novosibirsk State University, ul. Pirogova 2, 630090 Novosibirsk, Russia; Institute of Computational Technologies, Siberian Branch, Russian Academy of Science, prosp. Akad. Lavrent'eva 6, 630090 Novosibirsk, Russia; e-mail: o.s.sidelnikov@gmail.com, mifester@gmail.com;
S. Sygletos, F. Ferreira Aston University, England, Birmingham, B4 7ET; e-mail: s.sygletos@aston.ac.uk; f.ferreira@scton.ac.uk

Received 17 April 2015; revision received 21 October 2015
Kvantovaya Elektronika **46** (1) 76–80 (2016)
Translated by V.L. Derbov

study the process of propagation of electromagnetic radiation in multimode fibres. As the basis model, we consider the model proposed in Refs [18, 19], based on the Manakov equations and describing the nonlinear propagation of the signal in multimode fibres. The aim of the present paper is to find the configuration of a digital communication system, optimal with respect to minimising the error vector magnitude (EVM), depending on the number of propagating modes and the modulation type. To compare different configurations we determine the bit-error rate (BER) and EVM as functions of the optical signal-to-noise ratio (OSNR).

2. Nonlinear propagation in multimode fibres

The electric field in a multimode fibre can be presented as a sum of the fields of M different spatial modes of the fibre in the frequency domain [18]

$$\tilde{E}(x,y,z,\omega) = \sum_{m}^{M} \exp(\mathrm{i}\beta_m(\omega)z)\tilde{A}_m(z,\omega)F_m(x,y)/\sqrt{N_m},$$

where $\tilde{A}_m(z,\omega) = [\tilde{A}_{mx}(z,\omega), \tilde{A}_{my}(z,\omega)]^{\mathrm{T}}$ is the Fourier transform of the field envelope in the time domain for the mth mode, including the amplitudes of both polarisation components of the spatial mode with the spatial distribution $F_m(x,y)$ and the propagation constant $\beta_m(\omega)$. The normalisation constant is $N_m = \frac{1}{3}\varepsilon_0 n_{\mathrm{eff}} c I_m$, where

$$I_m = (n_m/n_{\mathrm{eff}}) \iint F_m^2(x,y)\mathrm{d}x\mathrm{d}y;$$

ε_0 is the vacuum permittivity; n_{eff} is the effective refractive index for the fundamental mode; n_m is the effective refractive index for the mth mode; and c is the speed of light.

In the present paper, we consider two important cases of signal propagation through multimode fibres that are of practical interest, the weak- and strong-coupling regimes. In the first regime, the linear coupling between the different spatial modes is weak compared to the coupling between the two polarisation components of one spatial mode. In the regime of strong coupling both types of coupling are of the same order. Practically, some spatial modes may be coupled weakly, while other modes may be coupled stronger.

In the case of weak coupling of modes, the nonlinear propagation of a signal carried by one mode of a multimode fibre is described by the Manakov equation [18]:

$$\frac{\partial \bar{A}_p}{\partial z} + \langle \delta\beta_{0p}\rangle \bar{A}_p + \langle \delta\beta_{1p}\rangle \frac{\partial \bar{A}_p}{\partial z} + \mathrm{i}\frac{\beta_{2p}}{2}\frac{\partial^2 \bar{A}_p}{\partial z} = \\ = \mathrm{i}\gamma\left(f_{pppp}\frac{8}{9}|\bar{A}_p|^2 + \sum_{m\neq p} f_{mmpp}\frac{4}{3}|\bar{A}_m|^2\right)\bar{A}_p, \quad (1)$$

where

$$\langle \delta\beta_{0p}\rangle = \frac{1}{2}(\beta_{px} + \beta_{py}) - \beta_0;$$

$$\langle \delta\beta_{1p}\rangle = \frac{1}{2}\left(\frac{\partial\beta_{px}}{\partial\omega}\Big|_{\omega_0} + \frac{\partial\beta_{py}}{\partial\omega}\Big|_{\omega_0}\right) - \beta_{1p};$$

β_{0p}, $\beta_{1p} = 1/v_{\mathrm{g}}$, β_{2p} is the propagation constant, inverse to the group velocity, and the group velocity dispersion of the pth spatial mode (it is assumed that the polarisation components of a spatial mode have different group velocities, but similar group velocity dispersions); $\gamma = \omega_0 n_2/(cA_{\mathrm{eff}})$ is the nonlinear parameter; n_2 is the nonlinear refractive index of the glass; A_{eff} is the effective area of the fundamental mode at the centre frequency ω_0; and

$$f_{lmnp} = \frac{A_{\mathrm{eff}}}{(I_l I_m I_n I_p)^{1/2}} \iint F_l F_m F_n F_p \mathrm{d}x\mathrm{d}y \quad (2)$$

is the coefficient of nonlinear coupling between the spatial modes.

In the strong-coupling regime, when the linear coupling between different spatial modes becomes comparable with the coupling between the polarisation components of each mode, the propagation equation takes the form [19]:

$$\frac{\partial A}{\partial z} + \frac{1}{v_{\mathrm{g}}}\frac{\partial A}{\partial t} + \mathrm{i}\frac{\bar{\beta}_2}{2}\frac{\partial^2 A}{\partial t^2} = \mathrm{i}\gamma\kappa|A|^2 A, \quad (3)$$

where

$$\kappa = \sum_{k\leqslant l}^{M} \frac{32}{2^{\delta_{kl}}} \frac{f_{kkll}}{6M(2M+1)};$$

$1/v_g = \mathrm{Tr}(B_1)/2M$ is the mean inverse group velocity; $\bar{\beta}_2 = \mathrm{Tr}(B_2)/2M$ is the mean dispersion of the group velocity; B_1 and B_2 are the diagonal matrices containing inverse group velocities and dispersion parameters of each mode; and δ_{kl} is the Kronecker symbol.

3. Results of numerical modelling

To solve propagation equations (1) and (3), we used the symmetric version of the split-step Fourier method (SSFM) that has the second order of accuracy with respect to the step of the evolution variable z. The propagation equations were solver numerically with the step 100 m. As shown by the test calculations, this step is optimal from the point of view of calculation speed and precision.

The aim of the work was to find the EVM for the systems of data transmission over large distances, based on the multimode fibre with a low value of the DGD, depending on the number of propagating modes, connection regime and modulation type. To transmit the data we used polarisation-division and wavelength-division multiplexing together with the quadrature phase-shift keying (QPSK) and 16-level quadrature amplitude modulation (16-QAM). To shape the pulse we used the filter with the raised cosine response and the roll-off factor 0.2. This allowed the reduction of the transmission bandwidth of the signal and the minimisation of intersymbol interference. Each signal consisted of 2^{15} symbols with 32 samples per symbol and was transmitted with the symbol rate R_{s} = 28.5 Gbaud. We used five spectral channels with 50 GHz channel spacing.

The data were transmitted via the multimode fibre with the optimal parameters for a low DGD [20], which supported the propagation of four modes (LP_{01}, LP_{11}, LP_{02} and LP_{21}). This fibre has a graded core with a cladding trench (GCCT), the profile of the refractive index is shown in Fig. 1. Analytically the refractive index profile is described as

$$n(\rho) = \begin{cases} n(0)[1 - \Delta n_{\mathrm{co}}(\rho/w_1)^{\varkappa}] \text{ at } |\rho| < w_1, \\ n_{\mathrm{cl}} \text{ at } w_1 < |\rho| < w_1 + w_2, \\ n_{\mathrm{cl}}(1 - \Delta n_{\mathrm{tr}}) \text{ at } w_1 + w_2 < |\rho| < w_1 + w_2 + w_3, \\ n_{\mathrm{cl}} \text{ at } |\rho| > w_1 + w_2 + w_3, \end{cases}$$

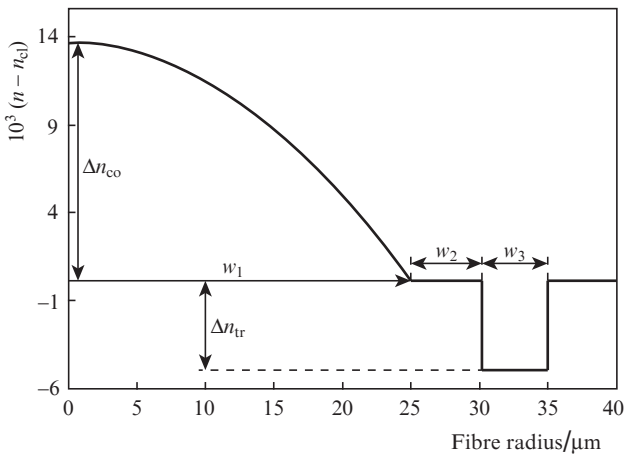

Figure 1. Profile of the refractive index of a fibre with GCCT.

where ρ is the fibre radius; n_{co}, n_{cl} and n_{tr} are the refractive indices of the core, cladding and trench, respectively; $\varkappa$ is the index of gradience; and w_1, w_2 and w_3 see in Fig. 1.

We considered the communication line 1000 km long, consisting of 10 spans, each 100 km long. The optical losses of the signal were compensated for by means of erbium-doped fibre amplifiers (EDFAs) placed after each span. The values of the DGD and the dispersion parameter D in each of the four modes are presented in Table 1, and the nonlinear coupling coefficients (2) of all modes in Table 2.

Table 1. Differential group delay and dispersion parameter for fibres with GCCT.

Mode	DGD/ps km^{-1}	D/ps km^{-1} nm^{-1}
LP_{01}	0	22.1758
LP_{11}	–5.1044	22.1526
LP_{02}	–5.0867	21.6334
LP_{21}	–5.1044	21.8935

Table 2. Nonlinear coupling coefficients for a fibre with GCCT (in W^{-1} km^{-1}).

Mode	LP_{01}	LP_{11}	LP_{02}	LP_{21}
LP_{01}	0.728304	0.361509	0.366151	0.182191
LP_{11}		0.540299	0.182238	0.272129
LP_{02}			0.365446	0.18328
LP_{21}				0.41122

The raised cosine-shaped signals output from the transmitter serve as the initial data for the solution of the propagation equations (1) and (3) using SSFM. To simulate the noises of the amplified spontaneous emission (ASE), generated by the EDFA, the complex modulated signal transmitted through the channel was artificially worsened at the line end before the receiver by introducing the additive white Gaussian noise (a random quantity with a zero mean value and the variance σ^2). The correctness of introducing the noise at the end of the channel is substantiated by the fact that the nonlinear coupling between the ASE and the signal is much weaker than the nonlinear interaction of the signal with itself [18]. The spectral density of the noise in the case of the EDFA is determined by the formula from [21]:

$$N_{\mathrm{ASE}}^{\mathrm{EDFA}} = N_{\mathrm{A}}[\exp(\alpha L_A) - 1]h\nu_{\mathrm{s}}n_{\mathrm{sp}},$$

where N_{A} is the number of amplifiers in the channel; α is the attenuation constant; L_{A} is the span length; h is the Planck constant; ν_{s} is the optical frequency; and n_{sp} is the coefficient of spontaneous radiation.

To study this system in the course of transmitting signals via different combinations of spatial modes in the regime of strong and weak coupling we calculated the BER and the parameter 1/EVM^2 as a function of the OSNR in each case and compared the obtained results. It is worth noting that in the case of QPSK signals the parameter 1/EVM^2 is equal to the Q^2 factor. To find BER and EVM we performed 1000 calculations with random noise realisation and calculated the median average of the obtained data. In this case, the mean square deviation of BER and EVM was of the order of 10^{-4}.

Figure 2 shows the dependence of the parameter 1/EVM^2 on the OSNR after the transmission of bit stream via a single mode using QPSK and 16-QAM. For comparison, the signal was separately input into each mode (LP_{01}, LP_{11}, LP_{02} and LP_{21}). Note that in this case QPSK and 16-QAM yield coincident results for the magnitude of the error vector. As seen from Fig. 2, the modes with smaller nonlinear coefficients (see Table 2) demonstrate smaller EVM, since in this case the nonlinear contribution in Eqns (1) and (3) decreases.

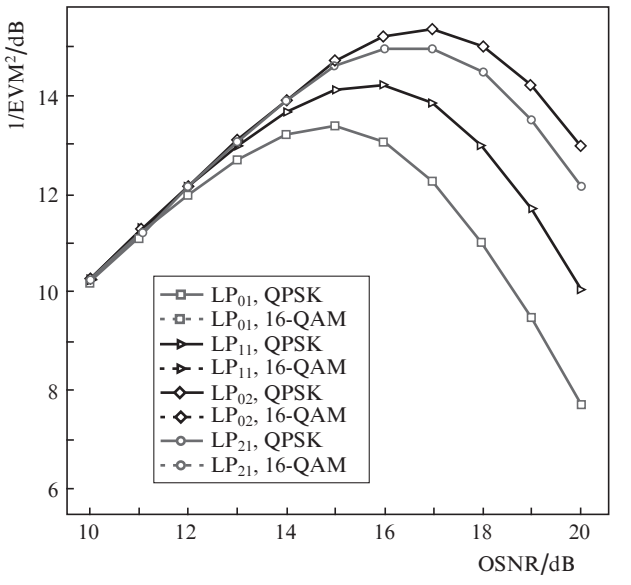

Figure 2. Dependence of 1/EVM^2 on the OSNR for the transmission of bit flows via one mode of a 1000-km-long multimode fibre.

Figure 3 shows the parameter 1/EVM^2 as a function of the OSNR for data transmission via the modes LP_{01} and LP_{11} under the conditions of strong and weak coupling with the use of QPSK and 16-QAM. We see that in this case the strong coupling of modes provides a smaller level of EVM as compared to EVM for weak coupling. The explanation is that the coefficient at the nonlinear part in the case of strong coupling (3) is smaller than that in the case of weak coupling (1).

Note that when we use the value DGD = –5 ps km^{-1} instead of DGD = –5.144 ps km^{-1} from Table 1, the parameter 1/EVM^2 increases in both cases of strong and weak mode cou-

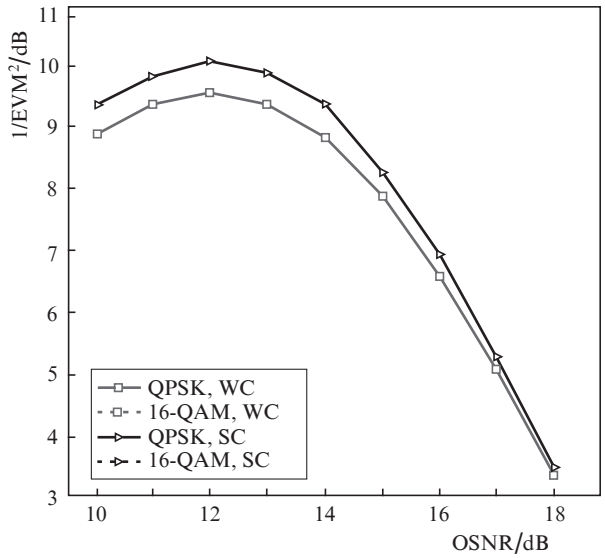

Figure 3. Dependence of $1/EVM^2$ on the OSNR for the transmission of bit flows via the modes LP_{01} and LP_{11} of a 1000-km-long multimode fibre under the conditions of strong (SC) and weak (WC) coupling.

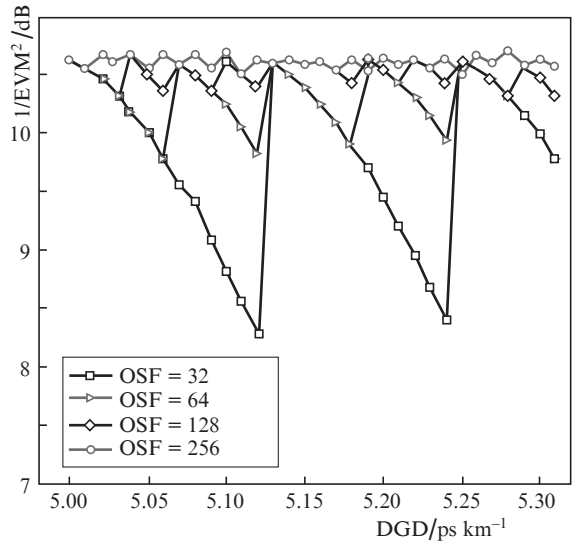

Figure 5. Dependence of $1/EVM^2$ on the differential group relay for different number of samples per symbol for the transmission of bit flows via the modes LP_{01} and LP_{11} of a 1000-km-long multimode fibre.

pling (Fig. 4). Thus, in our case the differential group delay can affect the magnitude of the error vector of the data transmission system.

Figure 5 shows the change in the parameter $1/EVM^2$ as a function of the DGD for a different number of samples per symbol (oversampling frequency, OSF) for the data transmission via two modes. In the present case OSNR=12 dB. It is seen that with the growth of OSF the parameter $1/EVM^2$ increases and becomes constant, i.e., for the sufficiently large number of samples per symbol the magnitude of the error vector stays unchanged under the variation of the DGD, and the resulting plots coincide with those of Fig 4. The possible explanation is that in the receiver the model numerically implements the compensation of signal time shift caused by the differential group delay. In the process of propagation through the channel with the length L the signal is time-shifted by $\beta_1 L$, and to compensate for this shift we should shift the signal back by $N_c = \beta_1 L \cdot \mathrm{OSF}/T_s$ samples (T_s being the period of the signal). However, as a rule this value is not integer, so that the signal shift by the integer number of samples closest to N_c does not provide full compensation of the signal shift caused by the differential group delay. The precision of this shift will grow with an increase in the number of samples per symbol.

Figure 6 demonstrates the parameter $1/EVM^2$ as a function of the OSNR when the signal is simultaneously transmit-

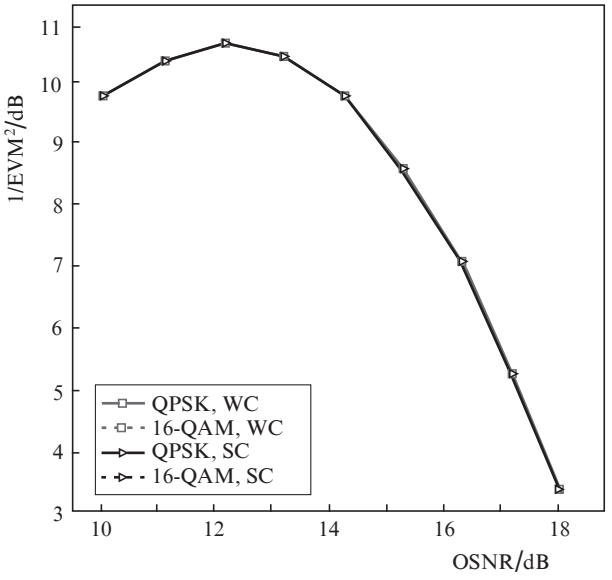

Figure 4. Dependence of the parameter $1/EVM^2$ on the OSNR for the transmission of data flows via two modes (LP_{01} and LP_{11}) of a 1000-km-long multimode fibre under the conditions of strong and weak coupling and DGD = –5 ps km^{-1}.

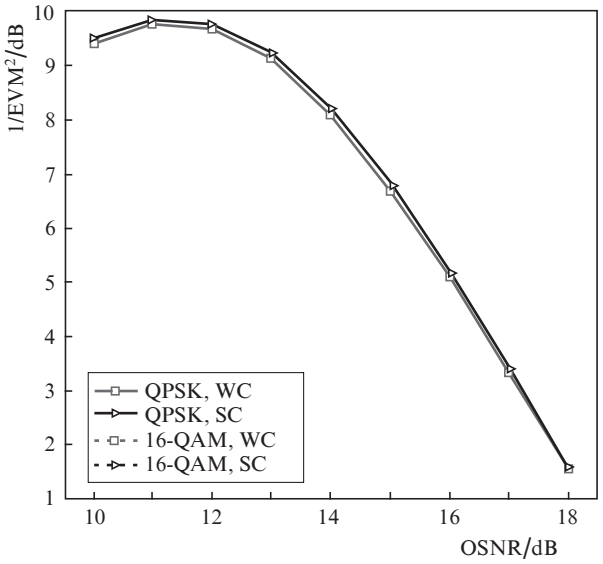

Figure 6. Dependence of $1/EVM^2$ on the OSNR for the transmission of bit flows simultaneously via four modes of a 1000-km-long multimode fibre under the conditions of strong (SC) and weak (WC) coupling.

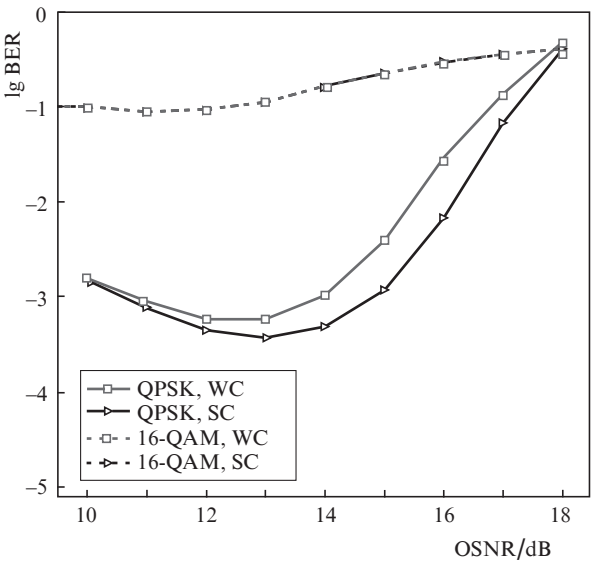

Figure 7. Dependence of BER on the OSNR after the transmission of bit flows via four modes of a 1000-km-long multimode fibre under the conditions of strong (SC) and weak (WC) coupling.

ted via all four modes. It is seen that with the increase in the number of active modes EVM grows, since the nonlinear contribution in Eqns (1) and (3) increases.

Figure 7 shows the dependence of BER on the OSNR for the data transmission via four modes. We see that here QPSK appears to be better than 16-QAM. Thus, we can conclude that for the appropriate parameters of the system of data transmission and forward error correction, one can achieve BER $\approx 10^{-10}$, which is enough for errorless data transmission in modern systems of digital communication.

4. Conclusions

The mathematical modelling of the evolution of electromagnetic radiation in multimode waveguides is carried out within the frameworks of a model, based on Manakov equations in the regimes of strong and weak coupling of modes. For this aim, a numerical algorithm based on the split-step Fourier method is implemented.

The parameter $1/\mathrm{EVM}^2$ has been found for a system of numerical communication based on a multimode fibre with a low differential group delay in the regimes of strong and weak mode coupling for the signal transmission via one, two and four modes. It is shown that EVM strongly depends on DGD if the number of samples per symbol is not large, and for sufficiently large OSF this dependence is practically absent. The growth of the system EVM under the increasing number of active modes is demonstrated. It is shown that with the growth of the number of modes the strong coupling regime provides a lower level of EVM than the weak coupling one. The possibility has been demonstrated of using multimode fibres with a low differential group delay for transmitting data in modern systems of digital communication.

Acknowledgements. The work was supported by the RF Ministry of Science and Education (Project RFMEFI57814X0029).

References

1. Qian D. In: *Proc. OFC/NFOEC 2011* (Los Angeles, 2011) PDPB5.
2. Zhou X. In: *Proc. OFC/NFOEC 2013* (Anaheim, 2013) OTu2B.4.
3. Yushko O.V., Nanii O.E., Redyuk A.A., et al. *Kvantovaya Elektron.*, **45** (1), 75 (2015) [*Quantum Electron.*, **45** (1), 75 (2015)].
4. Redyuk A.A. et al. *Laser Phys. Lett.*, **12**, 1 (2015).
5. Ryf R., Randel S., Gnauck A.H., et al. In: *Proc. OFC/NFOEC 2011* (Los Angeles, 2011) PDPB10.
6. Ip E. et al. In: *Proc. ECOC 2011* (Geneva, 2011) Th.13.C.2.
7. Zhu B. *Opt. Express*, **19**, 17 (2011).
8. Sakaguchi J. et al. *J. Lightwave Technol.*, **31**, 4 (2013).
9. Takara H. et al. In: *Proc. ECOC 2012* (Amsterdam, 2012) Th.3.C.1.
10. Appaiah K. et al. In: *Proc. ICC 2012* (Ottawa, 2012) p. 2972.
11. Liu J. et al. *Opt. Express*, **22**, 6 (2014).
12. Leunga A. et al. *Sens. Actuators B: Chem.*, **125**, 2 (2007).
13. Islam M. et al. *Sensors*, **14**, 4 (2014).
14. Carpenter J. *Opt. Express*, **22**, 3 (2014).
15. Inan B. et al. In: *Proc. OFC/NFOEC 2012* (Los Angeles, 2012) OW3D.4.
16. Gruner-Nielsen L. et al. In: *Proc. OFC/NFOEC 2012* (Los Angeles, 2012) PDP5A.1.
17. Ryf R. et al. In: *Proc. ECOC 2011* (Geneva, 2011) Th.13.C.1.
18. Mumtaz S. et al. *J. Lightwave Technol.*, **31**, 3 (2013).
19. Mecozzi A. et al. *Opt. Express*, **20**, 11 (2012).
20. Ferreira F.M. et al. *J. Lightwave Technol.*, **32**, 3 (2014).
21. Essiambre R.J. et al. *J. Lightwave Technol.*, **28**, 4 (2010).